
1 **Attribution of growing season evapotranspiration variability**
2 **considering snowmelt and vegetation changes in the arid alpine**
3 **basins**

4 Tingting Ning^{abc}, Zhi Li^d, Qi Feng^{ac*}, Zongxing Li^{ac} and Yanyan Qin^b

5 *^aKey Laboratory of Ecohydrology of Inland River Basin, Northwest Institute of Eco-Environment and Resources,*
6 *Chinese Academy of Sciences, Lanzhou, 730000, China*

7 *^bKey Laboratory of Land Surface Process and Climate Change in Cold and Arid Regions, Chinese Academy of*
8 *Sciences, Lanzhou 730000, China*

9 *^cQilian Mountains Eco-environment Research Center in Gansu Province, Lanzhou, 730000, China*

10 *^dCollege of Natural Resources and Environment, Northwest A&F University, Yangling, Shaanxi, 712100, China*

11 * Correspondence to: Qi Feng (qifeng@lzb.ac.cn)

12

13 **Abstract:** Previous studies have successfully applied variance decomposition
14 frameworks based on the Budyko equations to determine the relative contribution of
15 variability in precipitation, potential evapotranspiration (E_0), and total water storage
16 changes (ΔS) to evapotranspiration variance (σ_{ET}^2) on different time-scales; however,
17 the effects of snowmelt (Q_m) and vegetation (M) changes have not been incorporated
18 into this framework in snow-dependent basins. Taking the arid alpine basins in the
19 Qilian Mountains in northwest China as the study area, we extended the Budyko
20 framework to decompose the growing season σ_{ET}^2 into the temporal variance and
21 covariance of rainfall (R), E_0 , ΔS , Q_m , and M . The results indicate that the
22 incorporation of Q_m could improve the performance of the Budyko framework on a
23 monthly scale; σ_{ET}^2 was primarily controlled by the R variance with a mean
24 contribution of 63%, followed by the coupled R and M (24.3%) and then the coupled
25 R and E_0 (14.1%). The effects of M variance or Q_m variance cannot be ignored
26 because they contribute to 4.3% and 1.8% of σ_{ET}^2 , respectively. By contrast, the
27 interaction of some coupled factors adversely affected σ_{ET}^2 , and the ‘out-of-phase’
28 seasonality between R and Q_m had the largest effect (-7.6%). Our methodology and
29 these findings are helpful for quantitatively assessing and understanding hydrological
30 responses to climate and vegetation changes in snow-dependent regions on a finer
31 time-scale.

32 **Keywords:** evapotranspiration variability; snowmelt; vegetation; attribution

33 **1 Introduction**

34 Actual evapotranspiration (ET) drives energy and water exchanges among the
35 hydrosphere, atmosphere, and biosphere (Wang et al., 2007). The temporal variability
36 in ET is, thus, the combined effect of multiple factors interacting across the
37 soil–vegetation–atmosphere interface (Katul et al., 2012; Xu and Singh, 2005).
38 Investigating the mechanism behind ET variability is also fundamental for
39 understanding hydrological processes. The basin-scale ET variability has been widely
40 investigated with the Budyko framework (Budyko, 1961, 1974); however, most
41 studies are conducted on long-term or inter-annual scales and cannot interpret the
42 short-term ET variability (e.g. monthly scales).

43 Short-term ET and runoff (Q_r) variance have been investigated recently for their
44 dominant driving factors (Feng et al., 2020; Liu et al., 2019; Wu et al., 2017; Ye et al.,
45 2015; Zeng and Cai, 2015; Zeng and Cai, 2016; Zhang et al., 2016a); to this end, an
46 overall framework was presented by Zeng and Cai (2015) and Liu et al. (2019). Zeng
47 and Cai (2015) decomposed the intra-annual ET variance into the variance/covariance
48 of precipitation (P), potential evapotranspiration (E_0), and water storage change (ΔS)
49 under the Budyko framework based on the work of Koster and Suarez (1999).
50 Subsequently, Liu et al. (2019) proposed a new framework to identify the driving
51 factors of global Q_r variance by considering the temporal variance of P , E_0 , ΔS , and
52 other factors such as the climate seasonality, land cover, and human impact. Although

53 the proposed framework performs well for the *ET* variance decomposition, further
54 research is necessary for considering additional driving factors and for studying
55 regions with unique hydrological processes.

56 The impact of vegetation change should first be fully considered when studying the
57 variability of *ET*. Vegetation change significantly affects the hydrological cycle
58 through rainfall interception, evapotranspiration, and infiltration (Rodriguez-Iturbe,
59 2000; Zhang et al., 2016b). Higher vegetation coverage increases *ET* and reduces the
60 ratio of Q_r to P (Feng et al., 2016). However, most of the existing studies on *ET*
61 variance decomposition either ignored the effects of vegetation change or did not
62 quantify its contributions. Vegetation change is closely related to the Budyko
63 controlling parameters, and several empirical relationships have been successfully
64 developed on long-term and inter-annual scales (Li et al., 2013; Liu et al., 2018;
65 Ning et al., 2020; Xu et al., 2013; Yang et al., 2009). However, the relationship
66 between vegetation and its controlling parameters on a finer time-scale has received
67 less attention. As such, it is important to quantitatively investigate the contribution of
68 vegetation change to *ET* variability on a finer time-scale.

69 Second, for snow-dependent regions, the short-term water balance equation was the
70 foundation of decomposing *ET*/or Q_r variance. Its general form can be expressed as:

71
$$P = ET + Q_r + \Delta S, \quad (1)$$

72 where P , including liquid (rainfall) and solid (snowfall) precipitation, is the total water
73 source of the hydrological cycle. But this equation is unsuitable for regions where the
74 land-surface hydrology is highly dependent on the winter mountain snowpack and
75 spring snowmelt runoff. It has been reported that annual Q_r originating from
76 snowmelt accounts for 20–70% of the total runoff, including west United States
77 (Huning and AghaKouchak, 2018), coastal areas of Europe (Barnett et al., 2005), west
78 China (Li et al., 2019b), northwest India (Maurya et al., 2018), south of the Hindu
79 Kush (Ragetti et al., 2015), and high-mountain Asia (Qin et al., 2020). In these
80 regions, the mountain snowpack serves as a natural reservoir that stores cold-season P
81 to meet the warm-season water demand (Qin et al., 2020; Stewart, 2009). Thus, the
82 water balance equation should be modified to consider the impacts of snowmelt on
83 runoff in short-term time scale:

$$84 \quad R + Q_m = ET + Q_r + \Delta S, \quad (2)$$

85 where R is the rainfall, and Q_m is the snowmelt runoff. Many observations and
86 modelling experiments have found that due to global warming, increasing
87 temperatures would induce earlier runoff in the spring or winter and reduce the flows
88 in summer and autumn (Barnett et al., 2005; Godsey et al., 2014; Stewart et al., 2005;
89 Zhang et al., 2015). Therefore, the role of snowmelt change on ET variability in
90 snow-dependent basins on a finer time-scale should be studied.

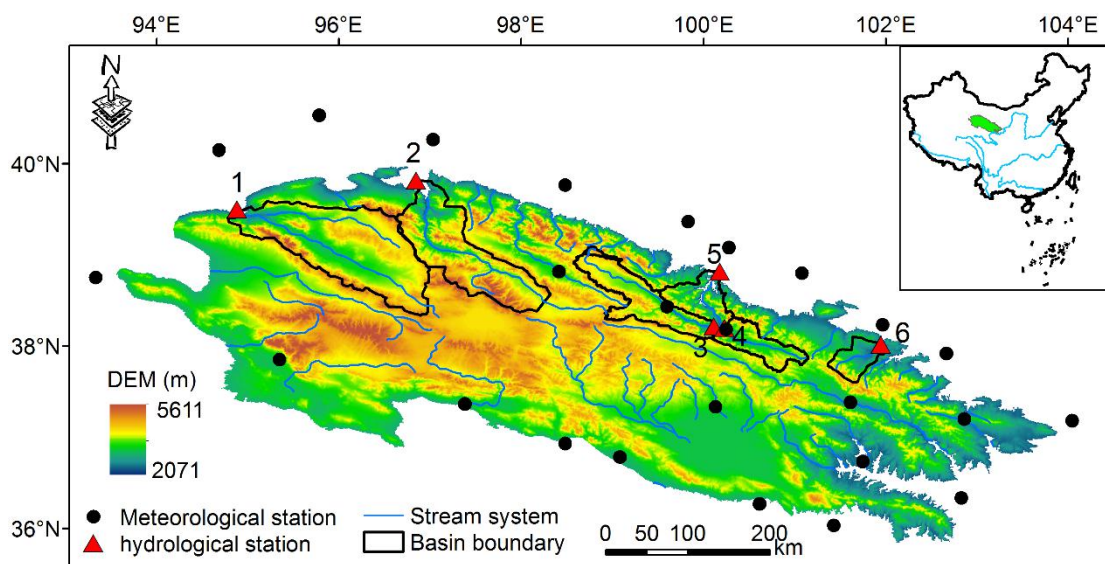
91 The overall objective of this study was to decompose the *ET* variance into the
92 temporal variability of multiple factors considering vegetation and snowmelt change.
93 The six cold alpine basins in the Qilian Mountains of northwest China were taken as
94 an example study area. Specifically, we aimed to: (i) determine the dominant driving
95 factor controlling the *ET* variance; (2) investigate the roles of vegetation and
96 snowmelt change in the variance; and (3) understand the interactions among the
97 controlling factors in *ET* variance. The proposed method will help quantify the
98 hydrological response to changes in snowmelt and vegetation in snowmelt-dependent
99 regions, and our results will prove to be insightful for water resource management in
100 other similar regions worldwide.

101 **2 Materials**

102 **2.1 Study area**

103 Six sub-basins located in the upper reaches of the Heihe, Shiyang, and Shule rivers in
104 the Qilian Mountains were chosen as the study area (Figure 1). They are important
105 inland rivers in the dry region of northwest China. The runoff generated from the
106 upper reaches contributes to nearly 70% of the water resources of the entire basin and
107 thus plays an important role in supporting agriculture, industry development, and
108 ecosystem maintenance in the middle and downstream rivers (Cong et al., 2017;
109 Wang et al., 2010a). Snowmelt and in-mountain-generated rainfall make up the water

110 supply system for the upper basins (Matin and Bourque, 2015), and the annual
111 average P exceeds 450 mm in this region. At higher altitudes, as much as 600–700
112 mm of P can be observed (Yang et al., 2017). Nearly 70% of the total rainfall
113 concentrates between June and September, while only 19% of the total rainfall occurs
114 from March to June. Snowmelt runoff is an important water source (Li et al., 2012; Li
115 et al., 2018; Li et al., 2016); in the spring, 70% of the runoff is supplied by snowmelt
116 water (Wang and Li, 2001). Characterised by a continental alpine semi-humid climate,
117 alpine desert glaciers, alpine meadows, forests, and upland meadows are the
118 predominant vegetation distribution patterns (Deng et al., 2013). Furthermore, this
119 region has experienced substantial vegetation changes and resultant hydrological
120 changes in recent decades (Bourque and Mir, 2012; Du et al., 2019; Ma et al., 2008).



122 Figure 1 The six basins in China's northern Qilian Mountains. The Digital elevation data, at
123 30 m resolution, was provided by the Geospatial Data Cloud site, Computer Network Information

124

125 **2.2 Data**

126 Daily climate data were collected for 25 stations distributed in and around the Qilian
127 Mountains from the China Meteorological Administration. They comprised rainfall,
128 air temperature, sunshine hours, and relative humidity and would be used to calculate
129 the monthly E_0 using the Priestley and Taylor (1972) equation.

130 The monthly runoff at the Dangchengwan, Changmabu, Zhamashike, Qilian,
131 Yingluoxia, and Shagousi hydrological stations were obtained for 2001–2014 from
132 the Bureau of Hydrology and Water Resources, Gansu Province. The sum of the
133 monthly soil moisture and plant canopy surface water with a resolution of $0.25^\circ \times$
134 0.25° from the Global Land Data Assimilation System (GLDAS) Noah model was
135 used to estimate the total water storage. The monthly ΔS was calculated as the water
136 storage difference between two neighbouring months. Eight-day composites of the
137 MODIS MOD10A2 Version 6 snow cover product from the MODIS TERRA satellite
138 were used to produce the monthly snow cover area (SCA) of each basin. The SCA data
139 were used to drive the snowmelt runoff model.

140 A monthly normalised difference vegetation index ($NDVI$) at a spatial resolution of 1
141 km from the MODIS MOD13A3.006 product was used to assess the vegetation
142 coverage (M), which can be calculated from the method of Yang et al. (2009):

143
$$M = \frac{NDVI - NDVI_{min}}{NDVI_{max} - NDVI_{min}} \quad (3)$$

144 where $NDVI_{max}$ and $NDVI_{min}$ are the $NDVI$ values of dense forest (0.80) and bare soil
145 (0.05).

146 ET from dataset of “ground truth of land surface evapotranspiration at regional scale
147 in the Heihe River Basin (2012-2016) ET_{map} Version 1.0” (hereafter “ ET_{map} ”), was
148 used to validate the reliability of our estimated ET . This dataset was published by
149 National Tibetan Plateau Data Center. It was upscaled from 36 eddy covariance flux
150 tower sites (65 site years) to the regional scale with five machine learning algorithms,
151 and then applied to estimate ET for each grid cell ($1 \text{ km} \times 1 \text{ km}$) across the Heihe
152 River Basin each day over the period 2012–2016. It has been evaluated to have high
153 accuracy (Xu et al., 2018). Basins 3,4,5 in our study belongs to the headwater
154 sub-basins of Heihe River, and our monthly ET from April to September during
155 2012-2014 was thus compared with ET_{map} .

156 **3 Methods**

157 **3.1 The Budyko framework at monthly scales**

158 Probing the ET variability in the growing season can provide basic scientific reference
159 points for agricultural activities and water resource planning and management (Li et
160 al., 2015; Wagle and Kakani, 2014). Thus, we focus on the growing season ET
161 variability on a monthly scale in this study.

162 Among the mathematical forms of the Budyko framework, this study employed the
163 function proposed by Choudhury (1999) and Yang et al. (2008) to assess the basin
164 water balance for good performance (Zhou et al., 2015):

$$165 \quad ET = \frac{P_e \times E_0}{(P_e^n + E_0^n)^{1/n}}, \quad (4)$$

166 where n is the controlling parameter of the Choudhury–Yang equation. P_e is the total
167 available water supply for ET . In previous studies, P_e included P and ΔS ($P_e = P - \Delta S$) on
168 finer time scale (Liu et al., 2019; Zeng and Cai, 2015; Zhang et al., 2016a). But
169 snowmelt runoff should also be considered in the snow-dependent basins. Thus, P_e
170 can be defined as:

$$171 \quad P_e = R + Q_s - \Delta S. \quad (5)$$

172 Equation 4 can thus be redefined as follows:

$$173 \quad ET_i = \frac{(R_i + Q_{s_i} - \Delta S_i) \times E_{0_i}}{((R_i + Q_{s_i} - \Delta S_i)^{n_i} + E_{0_i}^{n_i})^{1/n_i}}, \quad (6)$$

174 where i indicates each month of the growing season (April to September). After
175 estimating the monthly ET of the growing season using Equation 2, the values of n for
176 each month can be obtained via Equation 6.

177 **3.2 Estimating the equivalent of snowmelt runoff**

178 With the developed relationship between snowmelt and air temperature (Hock, 2003),

179 the degree-day model simplifies the complex processes and performs well, so it is
180 widely used in snowmelt estimation (Griessinger et al., 2016; Rice et al., 2011;
181 Semadeni-Davies, 1997; Wang et al., 2010a). This study estimated the monthly Q_s
182 using the degree-day model following the Wang et al. (2015) procedure. Specifically,
183 the water equivalent of snowmelt (W , mm) during the period m can be calculated as:

$$184 \quad \sum_{i=1}^m W_i = DDF \sum_{i=1}^m T_i^+, \quad (7)$$

185 where DDF denotes the degree-day factor ($\text{mm/day} \cdot ^\circ \text{C}$), and T^+ is the sum of the
186 positive air temperatures of each month. After obtaining W , the monthly Q_s of each
187 elevation zone can be expressed as:

$$188 \quad \sum_{i=1}^m Q_{Si} = \sum_{i=1}^m W_i SCA_i, \quad (8)$$

189 where SCA_i is the snow cover area of each elevation zone.

190 According to Gao et al. (2011), the DDF values of Basins 1–6 were set to 3.4, 3.4, 4.0,
191 4.0, 4.0, and 1.7 $\text{mm/day} \cdot ^\circ \text{C}$, respectively. The six basins were divided into seven
192 elevation zones with elevation differences of 500 m. The sum of Q_s in each elevation
193 zone could be considered as the total Q_s of each basin. Previous studies have found
194 that the major snow melting period is from March to July in this area (Wang and Li,
195 2005; Wu et al., 2015); furthermore, the MODIS snow product also showed that the
196 SCA decreased significantly at the end of July. Thus, the snowmelt runoff from April

197 to July for the growing season was estimated in this study.

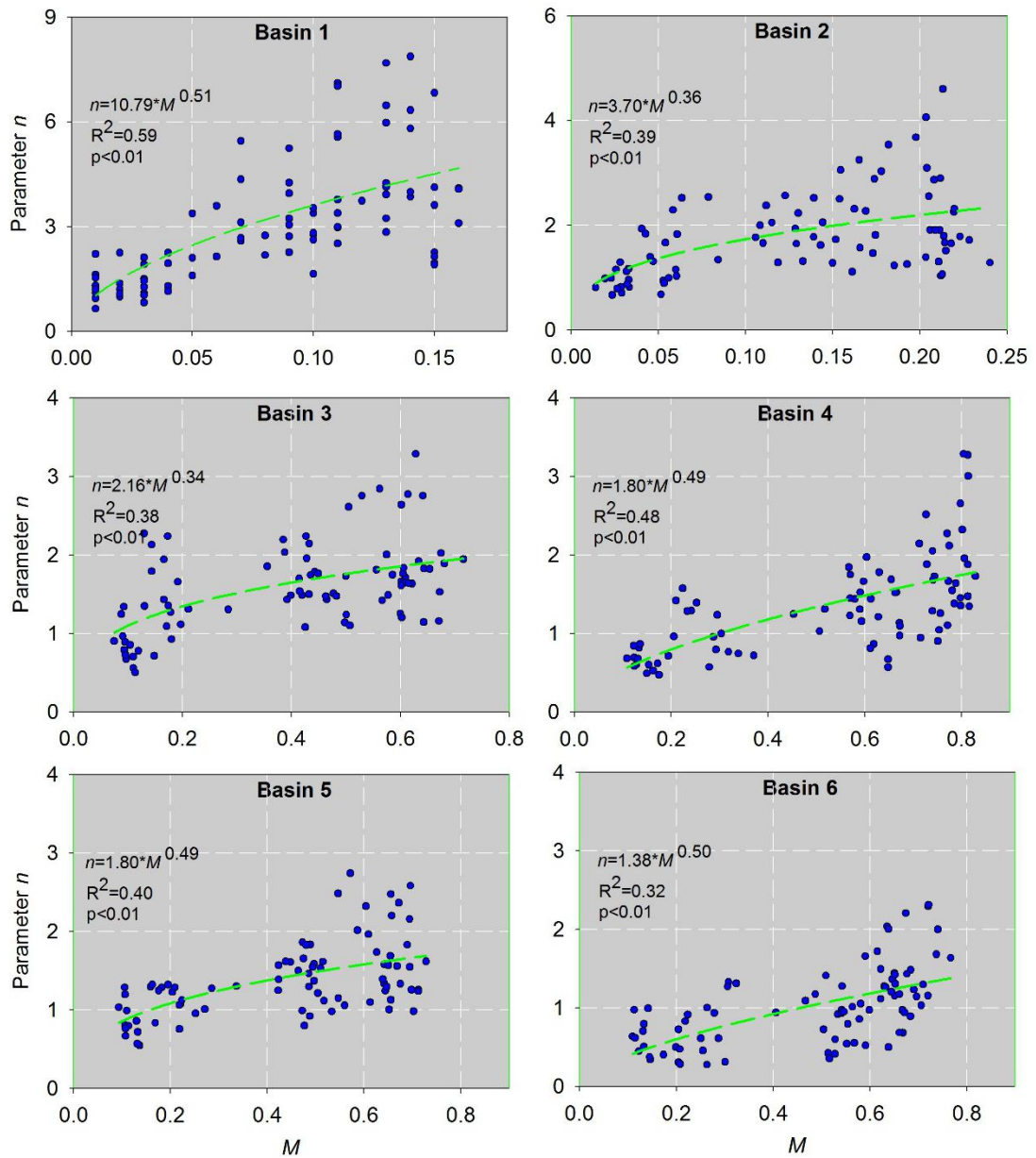
198 **3.3 Relationship between the Budyko controlling parameter and vegetation**
199 **change**

200 The relationships between the monthly parameters n and M for each basin in the
201 growing season for 2001–2014 are presented in Figure 2. It can be seen that parameter
202 n was significantly positively related to M in all six basins ($p < 0.05$), which means
203 that ET increased with increasing vegetation conditions under the given climate
204 conditions.

205 In Equation 6, when $n \rightarrow 0$, $ET \rightarrow 0$, which means M should have the following limiting
206 conditions: if $ET \rightarrow 0$, $T \rightarrow 0$ (transpiration), and thus $M \rightarrow 0$. Considering the
207 relationship shown in Figure 2 and the above limiting conditions, the general form of
208 parameter n can be expressed by power function followed previous studies (Liu et al.,
209 2018; Ning et al., 2017; Yang et al., 2007):

210
$$n = a \times M^b, \quad (9)$$

211 where a and b are constants, and their specific values for each basin are fitted in
212 Figure 2.



213

214 Figure 2 Relationships between the parameter n and the vegetation coverage for each basin on a

215

monthly scale.

216 3.4 ET variance decomposition

217 Liu et al. (2019) proposed a framework to identify the driving factors behind the

218 temporal variance of Q_r by combining the unbiased sample variance of Q_r with the

219 total differentiation of Q_r changes. Here, we extended this method by considering the
 220 effects of changes in snowmelt runoff and vegetation coverage on ET variance.

221 By combining Equation 6 with Equation 9, Equation 6 can be simplified as $ET \approx f(R_i,$
 222 $Q_{mi}, \Delta S_i, E_{0i}, M_i)$. Thus, the total differentiation of ET changes can be expressed as:

$$223 \quad dET_i = \frac{\partial f}{\partial R} dR_i + \frac{\partial f}{\partial Q_s} dQ_{mi} + \frac{\partial f}{\partial \Delta S} d\Delta S_i + \frac{\partial f}{\partial E_0} dE_{0i} + \frac{\partial f}{\partial M} dM_i + \tau, \quad (10)$$

224 where τ is the error. $\frac{\partial f}{\partial R}$, $\frac{\partial f}{\partial Q_m}$, $\frac{\partial f}{\partial \Delta S}$, $\frac{\partial f}{\partial E_0}$, $\frac{\partial f}{\partial M}$ are the partial differential coefficients of
 225 ET to R , Q_m , ΔS , E_0 and M , respectively, which can be calculated as:

$$226 \quad \frac{\partial ET}{\partial R} = \frac{\partial ET}{\partial Q_m} = -\frac{\partial ET}{\partial \Delta S} = \frac{ET}{P_e} \times \left(\frac{E_0^n}{P_e^n + E_0^n} \right), \quad (11a)$$

$$227 \quad \frac{\partial ET}{\partial E_0} = \frac{ET}{E_0} \times \left(\frac{P_e^n}{P_e^n + E_0^n} \right), \quad (11b)$$

$$228 \quad \frac{\partial ET}{\partial M} = \frac{ET}{n} \left(\frac{\ln(P_e^n + E_0^n)}{n} - \frac{P_e^n \ln P_e + E_0^n \ln E_0}{P_e^n + E_0^n} \right) \times a \times b \times M^{b-1}. \quad (11c)$$

229 The first-order approximation of ET changes in Equation 10 can be expressed as:

$$230 \quad \Delta ET_i \approx \varepsilon_1 \Delta R_i + \varepsilon_2 \Delta Q_{s_i} + \varepsilon_3 \Delta S_i + \varepsilon_4 \Delta E_{0_i} + \varepsilon_5 \Delta M_i, \quad (12)$$

231 where $\varepsilon_1 = \frac{\partial ET}{\partial R}$; $\varepsilon_2 = \frac{\partial ET}{\partial Q_s}$; $\varepsilon_3 = \frac{\partial ET}{\partial \Delta S}$; $\varepsilon_4 = \frac{\partial ET}{\partial E_0}$; $\varepsilon_5 = \frac{\partial ET}{\partial M}$.

232 The unbiased sample variance of ET is defined as:

$$233 \quad \sigma_{ET}^2 = \frac{1}{N-1} \sum_{i=1}^N (ET_i - \overline{ET})^2 = \frac{1}{N-1} \sum_{i=1}^N (\Delta ET_i)^2. \quad (13)$$

234 where \overline{ET} is the long term monthly mean of ET . N is the sample size, it equals 84 in
 235 this study (6 months/year×14 years=84 months). i is used to index time series of
 236 month from 1 to N .

237 Combining Equation 12 with Equation 13, σ_{ET}^2 can be decomposed as the
 238 contribution from different variance/covariance sources:

$$239 \quad \sigma_{ET}^2 = \sum_{i=1}^N (\varepsilon_1 \Delta R_i + \varepsilon_2 \Delta Q_{s_i} + \varepsilon_3 \Delta S_i + \varepsilon_4 \Delta E_{0_i} + \varepsilon_5 \Delta M_i)^2. \quad (14)$$

240 Expanding Equation 14, σ_{ET}^2 can be further rewritten as:

$$\begin{aligned} 241 \quad \sigma_{ET}^2 = & \varepsilon_1^2 \sigma_R^2 + \varepsilon_2^2 \sigma_{Q_s}^2 + \varepsilon_3^2 \sigma_{\Delta S}^2 + \varepsilon_4^2 \sigma_{E_0}^2 + \varepsilon_5^2 \sigma_M^2 + 2\varepsilon_1 \varepsilon_2 \text{cov}(R, Q_s) + \\ 242 \quad & 2\varepsilon_1 \varepsilon_3 \text{cov}(R, \Delta S) + 2\varepsilon_1 \varepsilon_4 \text{cov}(R, E_0) + 2\varepsilon_1 \varepsilon_5 \text{cov}(R, M) + 2\varepsilon_2 \varepsilon_3 \text{cov}(Q_s, \Delta S) + \\ 243 \quad & 2\varepsilon_2 \varepsilon_4 \text{cov}(Q_s, E_0) + 2\varepsilon_2 \varepsilon_5 \text{cov}(Q_s, M) + 2\varepsilon_3 \varepsilon_4 \text{cov}(E_0, \Delta S) + 2\varepsilon_3 \varepsilon_5 \text{cov}(M, \Delta S) + \\ 244 \quad & 2\varepsilon_4 \varepsilon_5 \text{cov}(E_0, M), \quad (15) \end{aligned}$$

245 where σ represents the standard deviation, and cov represents the covariance.

246 Equation 15 can be further simplified as:

$$\begin{aligned} 247 \quad \sigma_{ET}^2 = & F(R) + F(Q_s) + F(\Delta S) + F(E_0) + F(M) + F(R_{Q_s}) + F(R_{\Delta S}) + \\ 248 \quad & F(R_{E_0}) + F(R_M) + F(Q_s_{\Delta S}) + F(Q_s_{E_0}) + F(Q_s_M) + F(\Delta S_{E_0}) + \\ 249 \quad & F(\Delta S_M) + F(E_0_M), \quad (16) \end{aligned}$$

250 Where F is the individual contributions of each factor; each two factors linked by

251 underscore represents the interaction effects between them.

252 By separating out Equation 16, the contribution of each factor to σ_{ET}^2 can be
253 calculated as:

$$254 \quad C(X_j) = \frac{F(X_j)}{\sigma_{ET}^2} \times 100\%, \quad (17)$$

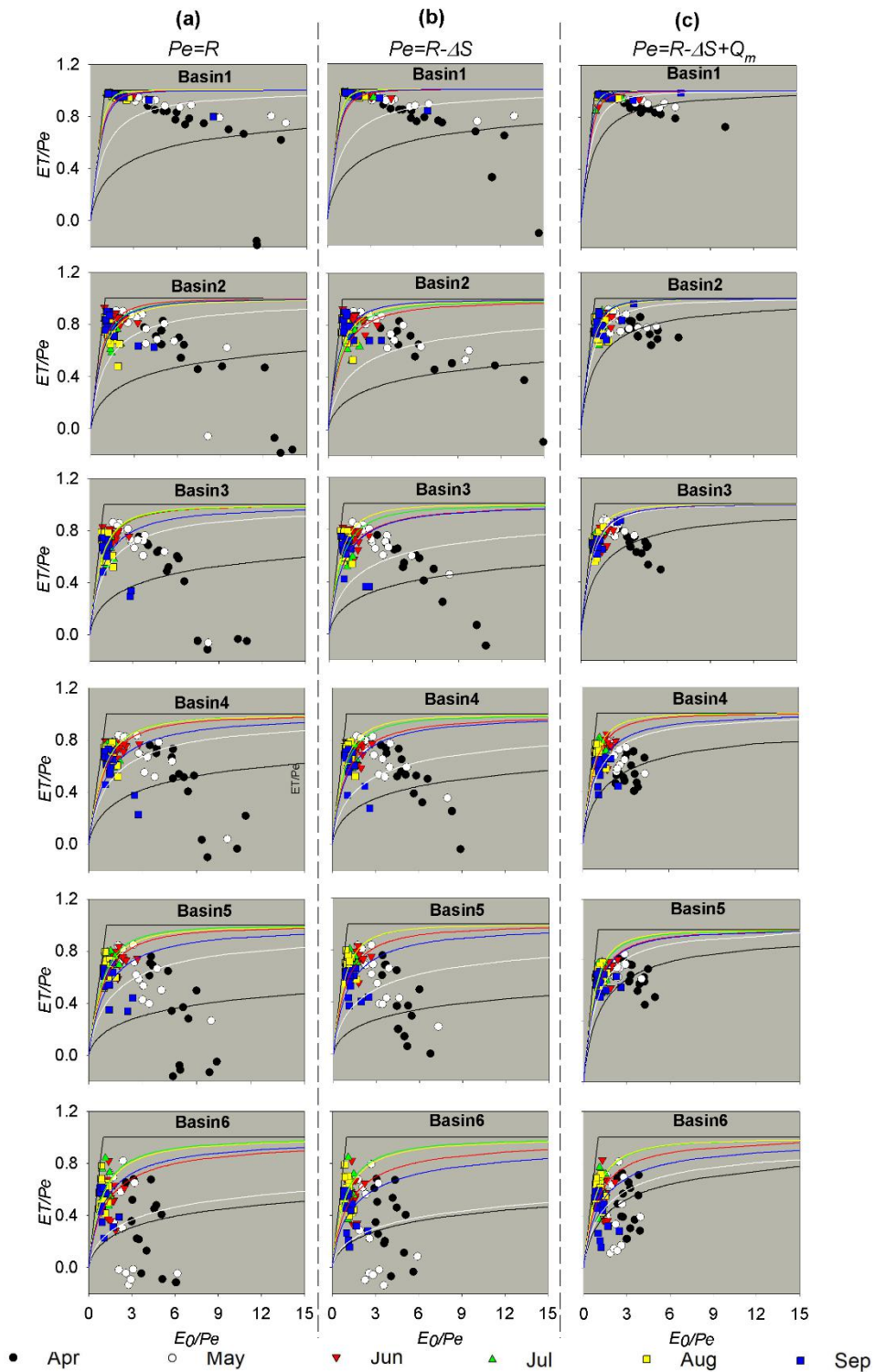
255 where $C(X_j)$ is the contribution of factor $F(j)$ to σ_{ET}^2 , and $j = 1-15$, representing the 15
256 factors in Equation 16.

257 **4 Results and Discussion**

258 **4.1 The effects of monthly storage change and snowmelt runoff in the Budyko** 259 **framework**

260 The Budyko framework is usually used for analyses of long-term average catchment
261 water balance; however, it was employed for the interpretation of the monthly
262 variability of the water balance in this study. Thus, it's very necessary to validate the
263 feasibility of Budyko equation for monthly variability. Furthermore, the impact of ΔS
264 on the representation of Budyko framework on a finer time-scale has been assessed
265 by several studies (Chen et al., 2013; Du et al., 2016; Liu et al., 2019; Zeng and Cai,
266 2015). However, the impact of Q_m and its combined effects with ΔS in
267 snowmelt-dependent basins are mostly ignored. Therefore, we present the water
268 balance in the monthly scale of six basins in the Budyko's framework with three

269 different computations of aridity index ($\phi=E_0/P_e$) or ET ratio (ET/P_e) in Figure 3. In
270 Figure 3a, $ET=R-Q_r$ when R is considered as water supply, i.e., $P_e=R$. The points of
271 monthly ET ratio and aridity index in April and May were well below Budyko curves
272 in 6 basins; monthly ET ratio was even negative in several year, which means the
273 local rain are not the only sources of ET in this area, especially in spring. In Figure 3b,
274 $ET=R-\Delta S-Q_r$ with $P_e=R-\Delta S$. Compared with figure 3a, the way-off points in April and
275 May were improved to a certain extent but negative points still existed, suggesting
276 that except for R , ΔS also play a significant role in maintaining spring ET , but the
277 variability of ET cannot be completely explained by these two variables. In Figure 3c,
278 $ET=R-\Delta S+Q_m-Q_r$ with $P_e=R-\Delta S+Q_m$. Compared to the points in Figures 3a-b, all
279 points focused on Budyko's curves more closely in each basin when $P_e=R+Q_m-\Delta S$.
280 From this comparison, it can be concluded that the Budyko framework is applicable to
281 the monthly scale in snowmelt-dependent basins, if the water supply is described
282 accurately by considering ΔS and Q_m .



283

284 Figure 3 Plots for the aridity index vs. evapotranspiration index scaled by the available water

285 supply for monthly series in the growing season. The total water availability is (a) R , (b) $R - \Delta S$,

286 (c) $R + Q_m - \Delta S$. The n value for each Budyko curve is fitted by long-term averaged monthly data.

287 4.2 Variations in the growing season water balance

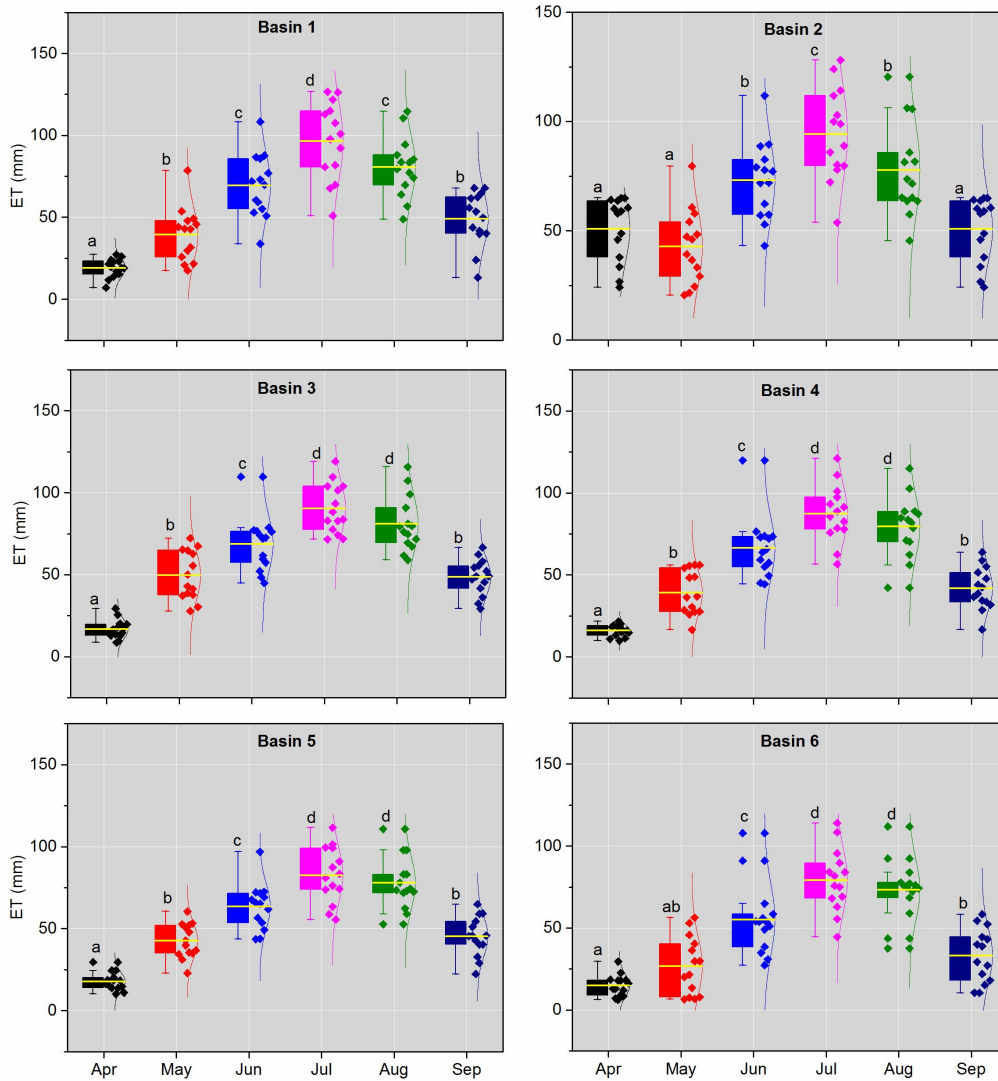
288 The mean and standard deviation (σ) for each item in the growing season water
289 balance in the six basins are summarised in Tables 1 and 2. The proportion of ΔS in
290 the water balance was small, with a mean value of 1.2 mm; however, its intra-annual
291 fluctuation was relatively large, with a $\sigma_{\Delta S}$ of 5.3 mm, and $\sigma_{\Delta S}$ was even as high as
292 9.0 mm in Basin 6. Compared to ΔS , Q_m represented a larger proportion of the water
293 balance with a mean of 8.5 ± 6.5 mm, indicating its important role in the basin water
294 supply. For this region, the water supply of ET was not only R but also included Q_m
295 and ΔS . Consequently, the mean monthly ET generally approached R (55.8 ± 27.4 mm)
296 or higher values in Basin 1.

297 Table 1 Averaged monthly hydrometeorological characteristics and vegetation coverage in the
298 growing season (2001–2014).

ID	Station	Area	R	Q_m	ΔS	E_0	M	n	E
1	Dangchengwan	14325	57.2	8.6	0.7	126.7	0.08	3.08	59.1
2	Changmabu	10961	68.9	10.8	1.1	123.0	0.13	1.79	59.3
3	Zhamashike	4986	73.5	10.6	1.5	120.3	0.40	1.59	59.1
4	Qilian	2452	74.5	9.0	1.4	116.8	0.44	1.37	54.9
5	Yingluoxia	10009	77.2	7.4	1.1	117.4	0.53	1.35	55.1
6	Shagousi	1600	83.5	4.8	1.4	116.3	0.48	1.01	47.1

299 The change patterns of the monthly R , ΔS , Q_m , and ET during the growing season are
300 presented in Figure 4 and Supplementary Figures S1–S3. R exhibited a regular
301 unimodal trend, with a maximum value occurring in July. The maximum Q_m appeared

302 in May, which is a result that is in agreement with previous studies in this region
303 (Wang and Qin, 2017; Zhang et al., 2016c). The peak of ΔS lagged that of Q_m for one
304 month in Basins 1–4 and three months in Basins 5–6, indicating a recharge of soil
305 water by snowmelt. Yang et al. (2015) also detected the time differences between ΔS
306 and Q_m and found that ΔS had a time lag of 3–4 months more than did Q_m in the Tarim
307 River Basin, another arid alpine basin in north-western China with hydroclimatic
308 conditions similar to those of the study region. Further, the abundant R in July should
309 contribute to more available water for ΔS ; however, the ΔS in July was relatively
310 small. This can be partially explained by the higher water consumption, i.e. the ET in
311 July. In a manner similar to the change pattern of R , ET exhibited a unimodal trend,
312 suggesting the crucial role of R .



313

314 Figure 4 Variations in the monthly *ET* for each basin during 2001–2014. A distribution curve is

315 shown to the right side of each box plot, and the data points are represented by diamonds.

316 Different letters indicate significant differences at $p < 0.05$.

317 4.3 Controlling factors of the *ET* variance

318 The contributions of R , E_0 , Q_m , ΔS , and M to σ_{ET}^2 for each basin are shown in Figure

319 5. The results showed that the variance of these five factors could explain σ_{ET}^2 , with

320 the total contribution rates ranging from 56.5% (Basin 6) to 98.6% (Basin 1). With the

321 decreasing ϕ from Basin 1 to Basin 6, $C(R)$ showed an increasing trend, ranging from
322 40.6% to 94.2%; conversely, $C(E_0)$ exhibited a decreasing trend, ranging from 0.2%
323 to 4.1%. This result indicated that R played a key role in σ_{ET}^2 in this region. Similarly,
324 Zhang et al. (2016a) found that $C(P)$ increased rapidly with increasing ϕ , whereas
325 $C(E_0)$ decreased rapidly based on 282 basins in China. Our results are also consistent
326 with previous conclusions that changes in ET or Q_r are dominated by changes in water
327 conditions rather than by energy conditions in dry regions (Berghuijs et al., 2017;
328 Yang et al., 2006; Zeng and Cai, 2016; Zhang et al., 2016a).

329 The M variance had the second largest contribution to σ_{ET}^2 with a mean $C(M)$ value
330 of 4.3% for the six basins. Specifically, $C(M)$ showed an increasing trend from 0.5%
331 to 9.5% with the decreasing ϕ , implying that the contribution of vegetation change to
332 ET variance was larger in relatively humid basin. It can be explained that transpiration
333 is more sensitive to vegetation change, and thus the higher vegetation coverage could
334 increase the proportion of transpiration to ET in humid regions (Niu et al., 2019;
335 Zhang et al., 2020). The Budyko hypothesis stated that change in ET is controlled by
336 change in available energy when water supply is not a limiting factor under humid
337 conditions (Budyko, 1974; Yang et al., 2006). The increasing M results in the
338 reallocation of available energy between canopy and soil. Specifically, more energy is
339 consumed by canopy thus increases transpiration. Further, Previous studies have
340 found that ET differs greatly among species, because of the difference in canopy

341 roughness, the timing of physiological functioning, water holding capacity of the soil
342 and rooting depth of the vegetation (Baldocchi et al., 2004; Bruemmer et al., 2012).
343 Generally, forest had larger ET than grassland (Ma et al., 2020; Zha et al., 2010). The
344 fraction of forest area is relatively high and thus lead to the higher contributions to ET
345 for whole basin in the humid region. For example, Wei et al. (2018) showed that the
346 global average variation in the annual Q_r due to the vegetation cover change was
347 $30.7\pm 22.5\%$ in forest-dominated regions on long-term scales, which was higher than
348 our results because of their higher forest cover.

349 The contribution of the Q_m variance ranked third with a mean value of 1.8%. Similar
350 as $C(R)$, $C(Q_m)$ showed a downward trend with the decreasing ϕ , ranging from 2.9%
351 to 0.4%. The larger $C(Q_m)$ can be explained by the larger variance in Q_m in Basins 2–4
352 (σ values in Table 2). However, the Q_m in Basin 1 was only 8.6 mm, and $C(Q_m)$ was
353 the largest in all six sub-basins (2.9%). It can be explained that the contribution of
354 each variable to σ_{ET}^2 was not only the product of the partial differential coefficients,
355 but also relied on its variance value according to Equation 14. Specifically, the partial
356 differential coefficients of 0.1 for a variable means that a 10% change in that variable
357 may result in a change in ET by 1%, which can only reflect the theoretical
358 contribution of each variable. By multiplying the variance value, the actual
359 contribution of each variable could be obtained. The ε_{Q_m} value was the largest in
360 Basin 1 and thus led to the largest $C(Q_m)$. In addition, shifts in the snowmelt period

361 can also partially explain the positive contribution of the Q_m variance. Like many
362 snow-dominated regions of the world (Barnett et al., 2005), climate warming shifted
363 the timing of snowmelt earlier in the spring in the Qilian Mountains (Li et al., 2012).
364 Earlier snowmelt due to a warmer atmosphere resulted in increased soil moisture and
365 a greater proportion of Q_m to ET (Barnhart et al., 2016; Bosson et al., 2012).

366 Previous studies have considered that most precipitation changes are transferred to
367 water storage (Wang and Hejazi, 2011); thus, ΔS has distinct impacts on the
368 intra-annual ET or Q_r variance in arid regions (Ye et al., 2015; Zeng and Cai, 2016;
369 Zhang et al., 2016a). However, the study region under investigation has a small $C(\Delta S)$
370 with a mean value of 1.02%, which is likely to be caused by the vegetation conditions
371 and time-scale. First, the six basins have higher vegetation coverage compared to
372 other arid basins; consequently, plant transpiration and rainfall interception consume
373 most of the water supply and reduce the transformation of rainfall to water storage.
374 This is consistent with previous studies that showed that the fractional contribution of
375 transpiration to ET would increase with increasing woody cover (Villegas et al., 2010;
376 Wang et al., 2010b). Second, the large contribution of ΔS to the intra-annual ET or Q_r
377 variance in arid regions is mostly detected at monthly scales. The smaller ΔS in the
378 non-growing season will increase the annual value of $\sigma_{\Delta S}$. However, this study
379 focused on the growing season with a smaller $\sigma_{\Delta S}$, which consequently led to a lower
380 $C(\Delta S)$.

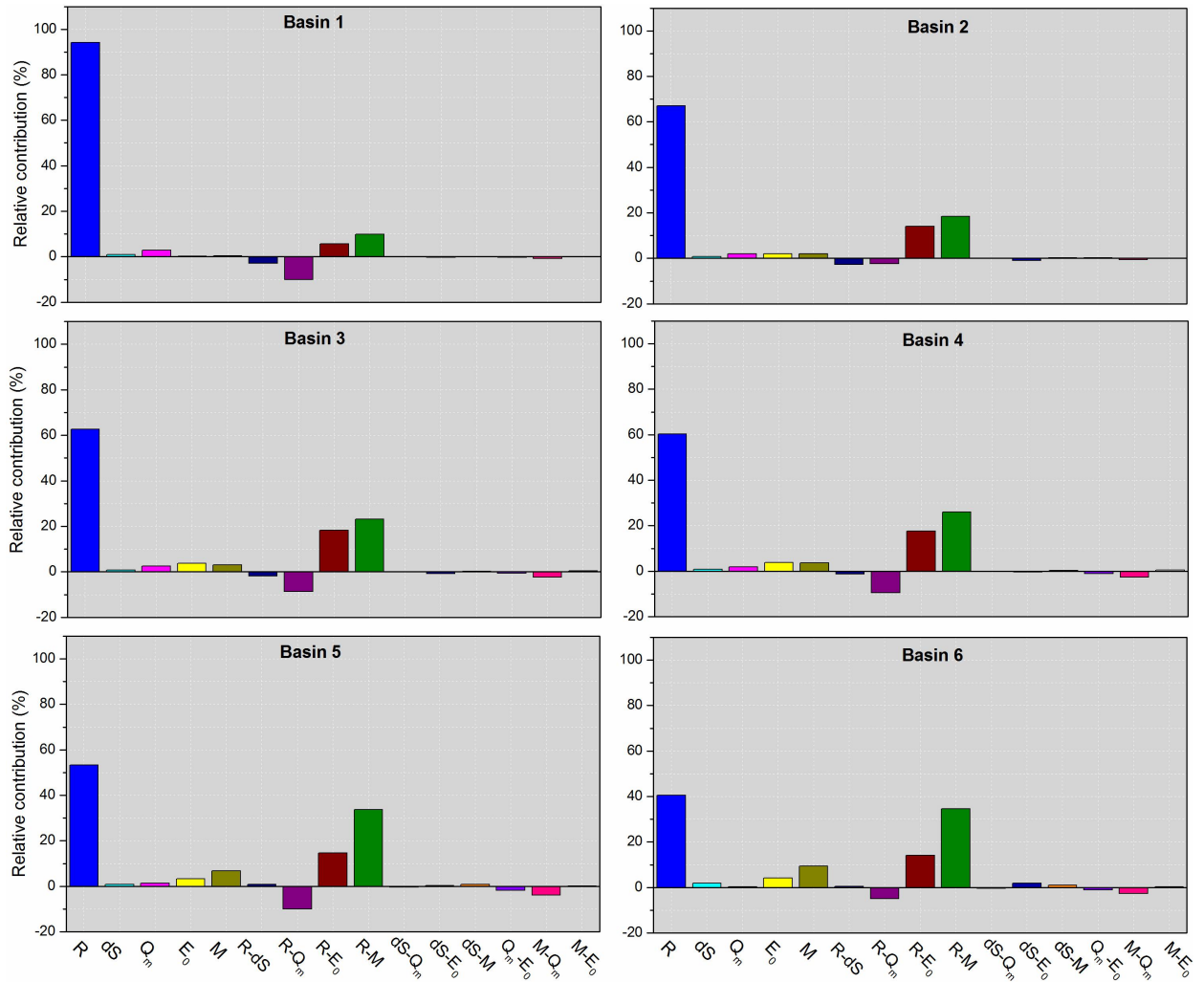
381 4.4 Interaction effects between controlling factors on the *ET* variance

382 The interaction effect of two factors on the *ET* variance was represented by their
383 covariance coefficients using Equations 15 and 16 (Figure 5). Among the ten groups
384 of interaction effects, the coupled *R* and *M* had the largest contribution to the *ET*
385 variance, with a mean value of 24.3%. The positive covariance of *R* and *M* indicated
386 that *M* changes in-phase with *R* (i.e. *R* occurred in the growing season), thus
387 increasing the *ET* variance. $C(R_M)$ showed an increasing trend from 9.9% to 34.6%
388 with decreasing ϕ . With different water conditions, the types and proportions of the
389 main ecosystems varied across basins. In particular, *F* showed an increasing trend
390 with decreasing ϕ , which partially explained the spatial variations in $C(R_M)$.
391 Previous studies concluded that the differences in physiological and phenological
392 characteristics of ecosystem types are likely to modulate the response of the
393 ecosystem *ET* to climate variability (Bruemmer et al., 2012; Falge et al., 2002; Li et
394 al., 2019a). For example, Yuan et al. (2010) found that, at the beginning of the
395 growing season, a significantly higher *ET* was observed in evergreen needleleaf
396 forests; however, during the middle term of the growing season (June–August), the
397 *ET* was largest in deciduous broadleaf forests in a typical Alaskan basin.

398 As an indicator of climate seasonality, the covariance of *R* and E_0 indicates matching
399 conditions between the water and energy supplies, such as the phase difference
400 between the storm season and warm season. A positive $\text{cov}(R, E_0)$ suggests an

401 in-phase R change with E_0 and consequently increases the ET variance. In this study,
402 following $C(R_M)$, the coupled R and E_0 had a large impact on the ET variance with a
403 mean contribution of 14.1%. With a typical temperate continental climate, the study
404 area has in-phase water and energy conditions; however, its ET is limited by the water
405 supply in spite of the abundant energy supply (Yang et al., 2006). The vegetation
406 receives the largest water supply in the growing season and can vary its biomass
407 seasonally in order to adapt to the R seasonality (Potter et al., 2005; Ye et al., 2016).
408 Consequently, the impact of climate variability on ET variance was mainly reflected
409 by the R seasonality in the study area.

410 In comparison, the interacting effects between R and Q_m , M and Q_m , R and ΔS , and Q_m
411 and E_0 contributed negatively to the ET variance. Among them, the effect of the
412 coupled R and Q_m was largest with a $C(R_Q_m)$ of -7.6% . This may suggest that Q_m
413 changes were out-of-phase with R . Specifically, the major snow melting period was
414 from March to May, when snowmelt water accounts for $\sim 70\%$ of the water supply;
415 however, $\sim 65\%$ of the annual R occurred in the summer (June–August) (Li et al.,
416 2019a). Overall, Q_m sustains the ET in the spring, but R supports the ET in the
417 summer.



418

419 Figure 5 Contribution to the *ET* variance in the growing season from each component in Equation

420

15.

421 **4.5 Uncertainties**

422 Uncertainties from different sources may result in errors for this study. First, this
 423 study estimated ΔS and Q_m with the GLDAS Noah land surface model and the
 424 degree-day model, respectively. Although the GLDAS ΔS has been widely used in
 425 hydrological studies, it ignores the change in deep groundwater (Nie et al., 2016; Syed

426 et al., 2008; Zhang et al., 2016), which may lead to errors in ET estimation based on
427 water balance equation. But previous studies showed that the groundwater change in
428 our study area is relatively small, and can thus be ignored. For example, Du et al.
429 (2016) used the abcd model to quantitatively determine monthly variations of water
430 balance for the sub-basins of Heihe River (including basins 3-5 in our study) and
431 found that the soil water storage change have obvious effects on the monthly water
432 balance, whilst the impact of monthly groundwater storage change is negligible.
433 Furthermore, it has been found that any change in climate conditions and underlying
434 basin characteristics will affect the contributions of heat balance components and
435 cause temporal variations of DDF (Kuusisto, 1980; Ohmura, 2001). But previous
436 studies indicated that there is no significant seasonal change in DDF in west China
437 (Zhang et al., 2006); as such, it is acceptable to estimate snowmelt runoff using fixed
438 DDF values in this study. In comparison, the contribution of snow meltwater to runoff
439 (F_s) was 12.9% in Basin 2 during 1971-2015 by using Spatial Processes in Hydrology
440 model(Li et al., 2019), while F_s was 25% in Basin 3 from 2001 to 2012 based on
441 geomorphology-based ecohydrological model (Li et al., 2018), <10% in Basin 6
442 during 1961-2006 by using SRM model (Gao et al., 2011). Our results indicated that
443 the F_s in Basin 2, 3 and 6 were 14.8%, 24.5% and 6.7%, respectively, which were
444 close to those from different models. Finally, the uncertainties of ΔS and Q_m may lead
445 to errors in ET estimation by water balance equation. To validate the reliability of our
446 estimated ET , the comparison with ET_{map} from April to September during 2012-2014

447 was conducted (Figure S4). The results showed that our estimated ET fitted well with
448 ET_{map} and basically fell around the 1:1 line, indicating ET estimated using water
449 balance equation by considering the items of ΔS and Q_m is acceptable.

450 Second, previous studies concluded that three main factors could be responsible for
451 the variability of n , including underlying physical conditions (such as soil and
452 topography characteristics) (Milly, 1994; Yang et al., 2009), climate seasonality (such
453 as the temporal variability of rainfall, mismatch between water and energy) (Ning et
454 al., 2017; Potter et al., 2005) and vegetation dynamics (Donohue et al., 2007; Zhang et
455 al., 2001). On the short time scale, the changes in soil and topography are negligible
456 and its impact on the variability of n can be ignored. In consequence, the factors,
457 should be considered, are climate seasonality and vegetation dynamics. When
458 parameterizing n , this study considered M but ignored climate seasonality since the
459 covariance item between R and E_0 , i.e. $\varepsilon_1 \varepsilon_4 \text{COV}(R, E_0)$ in the Equation (15) can
460 represent climate seasonality. In addition, human influence represented by parameter
461 n on the water balance cannot be ignored, which remains further investigation.

462 **5 Conclusion**

463 Recently, several studies have applied a variance decomposition framework based on
464 the Budyko equation to elucidate the dominant driving factors of the ET variance at
465 annual and intra-annual scales by decomposing the intra-annual ET variance into the

466 variance/covariance of P , E_0 , and ΔS . Vegetation changes can greatly affect the ET
467 variability, but their effects on the ET variance on finer time-scales was not quantified
468 by this decomposed method. Further, in snow-dependent regions, snowpack stores
469 precipitation in winter and releases water in spring; thus, Q_m plays an important role
470 in the hydrological cycle. Therefore, it is also necessary to consider the role of the Q_m
471 changes on the ET variability.

472 In this study, six arid alpine basins in the Qilian Mountains of northwest China were
473 chosen as examples. The monthly Q_m during 2001–2014 was estimated using the
474 degree-day model, and the growing season ET was calculated using the water balance
475 equation ($ET = R + Q_s - Q_r - \Delta S$). The controlling parameter n of the
476 Choudhury–Yang equation was found to be closely correlated with M , as estimated by
477 $NDVI$ data. Thus, by combining the Choudhury–Yang equation with the
478 semi-empirical formula between n and M , the growing season σ_{ET}^2 is decomposed
479 into the temporal variance and covariance of R , E_0 , ΔS , Q_m , and M . The main results
480 showed that considering Q_m and ΔS in the water balance equation can improve the
481 performance of the Budyko framework in snow-dependent basins on a monthly scale;
482 σ_{ET}^2 was primarily enhanced by the R variance, followed by the coupled R and M and
483 then the coupled R and E_0 . The enhancing effects of the variance in M and Q_m cannot
484 be ignored; however, the interactions between R and Q_m , M and Q_m , R and ΔS , and Q_m
485 and E_0 dampened σ_{ET}^2 . As a simple and effective method, our extended ET variance

486 decomposition method has the potential to be widely used to assess the hydrological
 487 responses to changes in the climate and vegetation in snow-dependent regions at finer
 488 time-scales.

489 Table 2 The elasticity coefficients of ET for five variables and the standard deviation of each
 490 variable for the six basins.

Basin	Elasticity coefficients					Standard deviation						
	ϵ_R	ϵ_{Q_m}	$\epsilon_{\Delta S}$	ϵ_{E_0}	ϵ_M	σ_R ,	σ_{Q_m} ,	$\sigma_{\Delta S}$,	σ_{E_0} ,	σ_M	Predicted	Assessed
						mm	mm	mm	mm		σ_{ET} , mm	σ_{ET} , mm
1	0.85	0.85	-0.85	0.06	41.94	34.4	6.0	3.4	25.5	0.05	30.2	31.2
2	0.56	0.56	-0.56	0.16	55.84	40.6	7.0	4.3	24.7	0.07	27.8	30.3
3	0.46	0.46	-0.46	0.20	20.81	42.5	8.5	4.9	23.6	0.21	24.9	27.9
4	0.44	0.44	-0.44	0.19	20.58	40.1	7.2	4.8	23.1	0.21	22.5	25.8
5	0.43	0.43	-0.43	0.19	24.60	39.8	6.3	5.1	22.0	0.25	23.3	25.0
6	0.33	0.33	-0.33	0.18	31.51	41.2	4.0	9.0	23.6	0.21	21.3	24.3

491

492

493 **Data availability**

494 The Digital elevation data are available at
495 <http://www.gscloud.cn/sources/accessdata/310?pid=302>. Meteorological data are
496 available at
497 [http://data.cma.cn/data/detail/dataCode/SURF_CLI_CHN_MUL_DAY_CES_V3.0.ht](http://data.cma.cn/data/detail/dataCode/SURF_CLI_CHN_MUL_DAY_CES_V3.0.html)
498 [ml](http://data.cma.cn/data/detail/dataCode/SURF_CLI_CHN_MUL_DAY_CES_V3.0.html). The runoff records were obtained from the Bureau of Hydrology and Water
499 Resources, Gansu Province. The GLDAS data are available at
500 https://disc.gsfc.nasa.gov/datasets/GLDAS_NOAH025_M_2.0/summary. MODIS
501 MOD10A2 Version 6 snow cover products are available at
502 <https://nsidc.org/data/mod10a2>. MODIS MOD13A3.006 products are available at
503 <https://lpdaac.usgs.gov/products/mod13a3v006/>. The dataset of “ground truth of land
504 surface evapotranspiration at regional scale in the Heihe River Basin (2012-2016)
505 ETmap Version 1.0” are available at
506 <http://data.tpdc.ac.cn/zh-hans/data/8efbb18d-bc02-4bf6-9f21-345480d6637f/?q=ETM>
507 [ap](http://data.tpdc.ac.cn/zh-hans/data/8efbb18d-bc02-4bf6-9f21-345480d6637f/?q=ETM).

508 **Author contributions**

509 Tingting Ning: Methodology, Writing–original draft, Software, Visualisation

510 Zhi Li: Writing–review & editing

511 Qi Feng: Conceptualisation, Supervision

512 Zongxing Li and Yanyan Qin: Data curation, Resources

513 **Competing interests**

514 The authors declare that they have no conflicts of interest.

515 **Acknowledgements**

516 This study was supported by the National Natural Science Foundation of China
517 (41807160), Opening Research Foundation of Key Laboratory of Land Surface
518 Process and Climate Change in Cold and Arid Regions, Chinese Academy of Sciences
519 (LPCC 2020003), the “Western Light”-Key Laboratory Cooperative Research
520 Cross-Team Project of Chinese Academy of Sciences, the CAS ‘Light of West China’
521 Program (Y929651001), the Major Program of the Natural Science Foundation of
522 Gansu Province, China (18JR4RA002) , and the Second Tibetan Plateau Scientific
523 Expedition and Research Program (STEP, Grant No.2019QZKK0405).

524 **References**

525 Baldocchi, D.D., Xu, L.K.,&Kiang, N., 2004. How plant functional-type, weather,
526 seasonal drought, and soil physical properties alter water and energy fluxes of

-
- 527 an oak-grass savanna and an annual grassland. *Agricultural and Forest*
528 *Meteorology*, 123(1-2): 13-39.
- 529 Barnett, T.P., Adam, J.C., & Lettenmaier, D.P., 2005. Potential impacts of a warming
530 climate on water availability in snow-dominated regions. *Nature*, 438(7066):
531 303-309.
- 532 Barnhart, T.B., Molotch, N.P., Livneh, B., Harpold, A.A., Knowles, J.F., & Schneider,
533 D., 2016. Snowmelt rate dictates streamflow. *Geophysical Research Letters*,
534 43(15): 8006-8016.
- 535 Berghuijs, W.R., Larsen, J.R., Van Emmerik, T.H.M., & Woods, R.A., 2017. A Global
536 Assessment of Runoff Sensitivity to Changes in Precipitation, Potential
537 Evaporation, and Other Factors. *Water Resources Research*, 53: 8475-8486.
- 538 Bosson, E., Sabel, U., Gustafsson, L.-G., Sassner, M., & Destouni, G., 2012. Influences
539 of shifts in climate, landscape, and permafrost on terrestrial hydrology.
540 *Journal of Geophysical Research-Atmospheres*, 117: D05120.
- 541 Bourque, C.P.A., & Mir, M.A., 2012. Seasonal snow cover in the Qilian Mountains of
542 Northwest China: Its dependence on oasis seasonal evolution and lowland
543 production of water vapour. *Journal of Hydrology*, 454: 141-151.
- 544 Bruemmer, C., Black, T.A., Jassal, R.S., Grant, N.J., Spittlehouse, D.L., Chen, B.,

545 Nesic, Z., Amiro, B.D., Arain, M.A., Barr, A.G., Bourque, C.P.A., Coursolle,
546 C., Dunn, A.L., Flanagan, L.B., Humphreys, E.R., Lafleur, P.M., Margolis,
547 H.A., McCaughey, J.H., & Wofsy, S.C., 2012. How climate and vegetation type
548 influence evapotranspiration and water use efficiency in Canadian forest,
549 peatland and grassland ecosystems. *Agricultural and Forest Meteorology*, 153:
550 14-30.

551 Budyko, M.I., 1961. Determination of evaporation from the land surface (in Russian).
552 *Izvestiya Akad.nauk Sssr.ser.geograf.geofiz*, 6: 3-17.

553 Budyko, M.I., 1974. *Climate and life*. Academic, New York.

554 Chen, X., Alimohammadi, N., & Wang, D., 2013. Modeling interannual variability of
555 seasonal evaporation and storage change based on the extended Budyko
556 framework. *Water Resources Research*, 49(9): 6067-6078.

557 Choudhury, B.J., 1999. Evaluation of an empirical equation for annual evaporation
558 using field observations and results from a biophysical model. *Journal of*
559 *Hydrology*, 216(1-2): 99-110.

560 Cong, Z., Shahid, M., Zhang, D., Lei, H., & Yang, D., 2017. Attribution of runoff
561 change in the alpine basin: a case study of the Heihe Upstream Basin, China.
562 *Hydrological Sciences Journal-Journal Des Sciences Hydrologiques*, 62(6):
563 1013-1028.

-
- 564 Deng, S., Yang, T., Zeng, B., Zhu, X., & Xu, H., 2013. Vegetation cover variation in the
565 Qilian Mountains and its response to climate change in 2000-2011. *Journal of*
566 *Mountain Science*, 10(6): 1050-1062.
- 567 Donohue, R.J., Roderick, M.L. and McVicar, T.R., 2007. On the importance of
568 including vegetation dynamics in Budyko's hydrological model. *Hydrology*
569 *and Earth System Sciences*, 11(2): 983-995.
- 570 Du, C., Sun, F., Yu, J., Liu, X., & Chen, Y., 2016. New interpretation of the role of
571 water balance in an extended Budyko hypothesis in arid regions. *Hydrology*
572 *and Earth System Sciences*, 20(1): 393-409.
- 573 Du, J., He, Z., Piatek, K.B., Chen, L., Lin, P., & Zhu, X., 2019. Interacting effects of
574 temperature and precipitation on climatic sensitivity of spring vegetation
575 green-up in arid mountains of China. *Agricultural and Forest Meteorology*,
576 269: 71-77.
- 577 Falge, E., Baldocchi, D., Tenhunen, J., Aubinet, M., Bakwin, P., Berbigier, P.,
578 Bernhofer, C., Burba, G., Clement, R., Davis, K.J., Elbers, J.A., Goldstein,
579 A.H., Grelle, A., Granier, A., Guomundsson, J., Hollinger, D., Kowalski, A.S.,
580 Katul, G., Law, B.E., Malhi, Y., Meyers, T., Monson, R.K., Munger, J.W.,
581 Oechel, W., Paw, K.T., Pilegaard, K., Rannik, U., Rebmann, C., Suyker, A.,
582 Valentini, R., Wilson, K., & Wofsy, S., 2002. Seasonality of ecosystem

583 respiration and gross primary production as derived from FLUXNET
584 measurements. *Agricultural and Forest Meteorology*, 113(1-4): 53-74.

585 Feng, S., Liu, J., Zhang, Q., Zhang, Y., Singh, V.P., Gu, X., & Sun, P., 2020. A global
586 quantitation of factors affecting evapotranspiration variability. *Journal of*
587 *Hydrology*, 584: 124688 .

588 Feng, X., Fu, B., Piao, S., Wang, S., & Ciais, P., 2016. Revegetation in China's Loess
589 Plateau is approaching sustainable water resource limits. *Nature Climate*
590 *Change*, 6: 1019-1022.

591 Gao, X., Zhang, S., Ye, B., & Gao, H., 2011. Recent changes of glacier runoff in the
592 Hexi Inland river basin. *Advances in Water Science (In Chinese)*, 22(3):
593 344-350.

594 Godsey, S.E., Kirchner, J.W., & Tague, C.L., 2014. Effects of changes in winter
595 snowpacks on summer low flows: case studies in the Sierra Nevada, California,
596 USA. *Hydrological Processes*, 28(19): 5048-5064.

597 Griessinger, N., Seibert, J., Magnusson, J., & Jonas, T., 2016. Assessing the benefit of
598 snow data assimilation for runoff modeling in Alpine catchments. *Hydrology*
599 *and Earth System Sciences*, 20(9): 3895-3905.

600 Hock, R., 2003. Temperature index melt modelling in mountain areas. *Journal of*

-
- 601 *Hydrology*, 282(1-4): 104-115.
- 602 Huning, L.S.,&AghaKouchak, A., 2018. Mountain snowpack response to different
603 levels of warming. *Proceedings of the National Academy of Sciences of the*
604 *United States of America*, 115(43): 10932-10937.
- 605 Katul, G.G., Oren, R., Manzoni, S., Higgins, C.,&Parlange, M.B., 2012.
606 Evapotranspiration: a process driving mass transport and energy exchange in
607 the soil-plant-atmosphere-climate system. *Reviews of Geophysics*, 50:
608 RG3002.
- 609 Koster, R.D.,&Suarez, M.J., 1999. A simple framework for examining the interannual
610 variability of land surface moisture fluxes. *Journal of Climate*, 12(7):
611 1911-1917.
- 612 Kuusisto, E., 1980. On the values and variability of degree-day melting factor in
613 Finland. *Nordic Hydrology*, 11(5): 235-242.
- 614 Lan, Y., Hu, X., Din, H., La, C.,&Song, J., 2012. Variation of Water Cycle Factors in
615 the Western Qilian Mountain Area under Climate Warming Taking the
616 Mountain Watershed of the Main Stream of Shule River Basin for Example.
617 *Journal of Mountain Science (in Chinese)* , 30(6): 675-680.
- 618 Li, B., Chen, Y., Chen, Z.,&Li, W., 2012. The Effect of Climate Change during

619 Snowmelt Period on Streamflow in the Mountainous Areas of Northwest
620 China. *Acta Geographica Sinica (In Chinese)* , 67(11): 1461-1470.

621 Li, D., Pan, M., Cong, Z., Zhang, L., & Wood, E., 2013. Vegetation control on water
622 and energy balance within the Budyko framework. *Water Resources Research*,
623 49(2): 969-976.

624 Li, H., Zhao, Q., Wu, J., Ding, Y., Qin, J., Wei, H., & Zeng, D., 2019. Quantitative
625 simulation of the runoff components and its variation characteristics in the
626 upstream of the Shule River. *Journal of Glaciology and Geocryology (in
627 Chinese)*, 41(4): 907-917.

628 Li, L.L., Li, J., Chen, H.M., & Yu, R.C., 2019a. Diurnal Variations of Summer
629 Precipitation over the Qilian Mountains in Northwest China. *Journal of
630 Meteorological Research*, 33(1): 18-30.

631 Li, S., Zhang, L., Kang, S., Tong, L., Du, T., Hao, X., & Zhao, P., 2015. Comparison of
632 several surface resistance models for estimating crop evapotranspiration over
633 the entire growing season in arid regions. *Agricultural and Forest
634 Meteorology*, 208: 1-15.

635 Li, X., Cheng, G., Ge, Y., Li, H., Han, F., Hu, X., Tian, W., Tian, Y., Pan, X., Nian, Y.,
636 Zhang, Y., Ran, Y., Zheng, Y., Gao, B., Yang, D., Zheng, C., Wang, X., Liu,
637 S., & Cai, X., 2018. Hydrological Cycle in the Heihe River Basin and Its

638 Implication for Water Resource Management in Endorheic Basins. *Journal of*
639 *Geophysical Research-Atmospheres*, 123(2): 890-914.

640 Li, Z., Feng, Q., Li, Z., Yuan, R., Gui, J.,&Lv, Y., 2019b. Climate background, fact
641 and hydrological effect of multiphase water transformation in cold regions of
642 the Western China: A review. *Earth-Science Reviews*, 190: 33-57.

643 Li, Z., Feng, Q., Wang, Q.J., Yong, S., Cheng, A.,&Li, J., 2016. Contribution from
644 frozen soil meltwater to runoff in an in-land river basin under water scarcity
645 by isotopic tracing in northwestern China. *Global and Planetary Change*, 136:
646 41-51.

647 Liu, J., Zhang, Q., Feng, S., Gu, X., Singh, V.P.,&Sun, P., 2019. Global Attribution of
648 Runoff Variance Across Multiple Timescales. *Journal of Geophysical*
649 *Research-Atmospheres*, 124(24): 13962-13974.

650 Liu, J., Zhang, Q., Singh, V.P., Song, C., Zhang, Y.,&Sun, P., 2018. Hydrological
651 effects of climate variability and vegetation dynamics on annual fluvial water
652 balance at global large river basins. *Hydrology & Earth System Sciences*, 22:
653 4047-4060.

654 Ma, S., Eichelmann, E., Wolf, S., Rey-Sanchez, C.,&Baldocchi, D.D., 2020.
655 Transpiration and evaporation in a Californian oak-grass savanna: Field
656 measurements and partitioning model results. *Agricultural and Forest*

-
- 657 *Meteorology*, 295: 108204.
- 658 Ma, Z., Kang, S., Zhang, L., Tong, L.,&Su, X., 2008. Analysis of impacts of climate
659 variability and human activity on streamflow for a river basin in arid region of
660 northwest China. *Journal of Hydrology*, 352(3-4): 239-249.
- 661 Matin, M.A.,&Bourque, C.P.A., 2015. Mountain-river runoff components and their
662 role in the seasonal development of desert-oases in northwest China. *Journal*
663 *of Arid Environments*, 122: 1-15.
- 664 Maurya, A.S., Rai, S.P., Joshi, N., Dutt, K.S.,&Rai, N., 2018. Snowmelt runoff and
665 groundwater discharge in Himalayan rivers: a case study of the Satluj River,
666 NW India. *Environmental Earth Sciences*, 77(19): 694.
- 667 Milly, P.C.D, 1994. Climate,soil-water storage, and the average annual water-balance.
668 *Water Resources Research*, 30(7): 2143-2156.
- 669 Nie, N., Zhang, W.C., Zhang, Z.J., Guo, H.D.,&Ishwaran, N., 2016. Reconstructed
670 Terrestrial Water Storage Change (Delta TWS) from 1948 to 2012 over the
671 Amazon Basin with the Latest GRACE and GLDAS Products. *Water*
672 *Resources Management*, 30(1): 279-294.
- 673 Ning, T., Li, Z. and Liu, W. , 2017. Vegetation dynamics and climate seasonality
674 jointly control the interannual catchment water balance in the Loess Plateau

675 under the Budyko framework. *Hydrology and Earth System Sciences*, 21(3):
676 1515-1526.

677 Ning, T., Li, Z., Feng, Q., Chen, W., & Li, Z., 2020. Effects of forest cover change on
678 catchment evapotranspiration variation in China. *Hydrological Processes*,
679 34(10): 2219-2228.

680 Niu, Z., He, H., Zhu, G., Ren, X., Zhang, L., Zhang, K., Yu, G., Ge, R., Li, P., Zeng,
681 N., & Zhu, X., 2019. An increasing trend in the ratio of transpiration to total
682 terrestrial evapotranspiration in China from 1982 to 2015 caused by greening
683 and warming. *Agricultural and Forest Meteorology*, 279: 107701 .

684 Ohmura, A., 2001. Physical basis for the temperature-based melt-index method.
685 *Journal of Applied Meteorology*, 40(4): 753-761.

686 Potter, N.J., Zhang, L., Milly, P.C.D., McMahon, T.A., & Jakeman, A.J., 2005. Effects
687 of rainfall seasonality and soil moisture capacity on mean annual water
688 balance for Australian catchments. *Water Resources Research*, 41(6): W06007.

689 Priestley, C., & Taylor, R., 1972. On the assessment of surface heat flux and
690 evaporation using large-scale parameters. *Monthly Weather Review*, 100(2):
691 81-92.

692 Qin, Y., Abatzoglou, J.T., Siebert, S., Huning, L.S., AghaKouchak, A., Mankin, J.S.,

693 Hong, C., Tong, D., Davis, S.J., & Mueller, N.D., 2020. Agricultural risks from
694 changing snowmelt. *Nature Climate Change*, 10(5): 459-465.

695 Ragetti, S., Pellicciotti, F., Immerzeel, W.W., Miles, E.S., Petersen, L., Heynen, M.,
696 Shea, J.M., Stumm, D., Joshi, S., & Shrestha, A., 2015. Unraveling the
697 hydrology of a Himalayan catchment through integration of high resolution in
698 situ data and remote sensing with an advanced simulation model. *Advances in*
699 *Water Resources*, 78: 94-111.

700 Rice, R., Bales, R.C., Painter, T.H., & Dozier, J., 2011. Snow water equivalent along
701 elevation gradients in the Merced and Tuolumne River basins of the Sierra
702 Nevada. *Water Resources Research*, 47: W08515.

703 Rodriguez-Iturbe, I., 2000. Ecohydrology: A hydrologic perspective of
704 climate-soil-vegetation dynamics. *Water Resources Research*, 36(1): 3-9.

705 Semadeni-Davies, A., 1997. Monthly snowmelt modelling for large-scale climate
706 change studies using the degree day approach. *Ecological Modelling*, 101(2-3):
707 303-323.

708 Stewart, I.T., 2009. Changes in snowpack and snowmelt runoff for key mountain
709 regions. *Hydrological Processes*, 23(1): 78-94.

710 Stewart, I.T., Cayan, D.R., & Dettinger, M.D., 2005. Changes toward earlier

711 streamflow timing across western North America. *Journal of Climate*, 18(8):
712 1136-1155.

713 Syed, T.H., Famiglietti, J.S., Rodell, M., Chen, J., & Wilson, C.R., 2008. Analysis of
714 terrestrial water storage changes from GRACE and GLDAS. *Water Resources
715 Research*, 44(2): W02433.

716 Villegas, J.C., Breshears, D.D., Zou, C.B., & Law, D.J., 2010. Ecohydrological controls
717 of soil evaporation in deciduous drylands: How the hierarchical effects of litter,
718 patch and vegetation mosaic cover interact with phenology and season.
719 *Journal of Arid Environments*, 74(5): 595-602.

720 Wagle, P., & Kakani, V.G., 2014. Growing season variability in evapotranspiration,
721 ecosystem water use efficiency, and energy partitioning in switchgrass.
722 *Ecohydrology*, 7(1): 64-72.

723 Wang, D., & Hejazi, M., 2011. Quantifying the relative contribution of the climate and
724 direct human impacts on mean annual streamflow in the contiguous United
725 States. *Water Resources Research*, 47: W00J12.

726 Wang, J., Li, H., & Hao, X., 2010a. Responses of snowmelt runoff to climatic change
727 in an inland river basin, Northwestern China, over the past 50 years.
728 *Hydrology and Earth System Sciences*, 14(10): 1979-1987.

-
- 729 Wang, J.,&Li, S., 2005. The influence of climate change on snowmelt runoff variation
730 in arid alpine regions of China. *Science in China (In Chinese)*, 35(7): 664-670.
- 731 Wang, J.,&Li, W., 2001. Establishing snowmelt runoff simulating model using remote
732 sensing data and GIS in the west of China. *International Journal of Remote*
733 *Sensing*, 22(17): 3267-3274.
- 734 Wang, K., Wang, P., Li, Z., Cribb, M.,&Sparrow, M., 2007. A simple method to
735 estimate actual evapotranspiration from a combination of net radiation,
736 vegetation index, and temperature. *Journal of Geophysical*
737 *Research-Atmospheres*, 112(D15): D15107.
- 738 Wang, L., Caylor, K.K., Villegas, J.C., Barron-Gafford, G.A., Breshears,
739 D.D.,&Huxman, T.E., 2010b. Partitioning evapotranspiration across gradients
740 of woody plant cover: Assessment of a stable isotope technique. *Geophysical*
741 *Research Letters*, 37: L09401.
- 742 Wang, R., Yao, Z., Liu, Z., Wu, S., Jiang, L.,&Wang, L., 2015. Snow cover variability
743 and snowmelt in a high-altitude ungauged catchment. *Hydrological Processes*,
744 29(17): 3665-3676.
- 745 Wang, Y.-J.,&Qin, D.-H., 2017. Influence of climate change and human activity on
746 water resources in arid region of Northwest China: An overview. *Advances in*
747 *Climate Change Research*, 8(4): 268-278.

-
- 748 Wei, X., Li, Q., Zhang, M., Giles-Hansen, K., Liu, W., Fan, H., Wang, Y., Zhou, G.,
749 Piao, S., & Liu, S., 2018. Vegetation cover-another dominant factor in
750 determining global water resources in forested regions. *Global Change*
751 *Biology*, 24(2): 786-795.
- 752 Wu, C., Hu, B.X., Huang, G., & Zhang, H., 2017. Effects of climate and terrestrial
753 storage on temporal variability of actual evapotranspiration. *Journal of*
754 *Hydrology*, 549: 388-403.
- 755 Wu, F., Zhan, J., Wang, Z., & Zhang, Q., 2015. Streamflow variation due to glacier
756 melting and climate change in upstream Heihe River Basin, Northwest China.
757 *Physics and Chemistry of the Earth*, 79-82: 11-19.
- 758 Xu, C.Y., & Singh, V.P., 2005. Evaluation of three complementary relationship
759 evapotranspiration models by water balance approach to estimate actual
760 regional evapotranspiration in different climatic regions. *Journal of Hydrology*,
761 308(1-4): 105-121.
- 762 Xu, T., Guo, Z., Liu, S., He, X., Meng, Y., Xu, Z., Xia, Y., Xiao, J., Zhang, Y., & Ma, Y.,
763 2018. Evaluating Different Machine Learning Methods for Upscaling
764 Evapotranspiration from Flux Towers to the Regional Scale. *Journal of*
765 *Geophysical Research: Atmospheres*, 123: 8674-8690.
- 766 Xu, X., Liu, W., Scanlon, B.R., Zhang, L., & Pan, M., 2013. Local and global factors

767 controlling water-energy balances within the Budyko framework. *Geophysical*
768 *Research Letters*, 40(23): 6123-6129.

769 Yang, D., Shao, W., Yeh, P.J.F., Yang, H., Kanae, S., & Oki, T., 2009. Impact of
770 vegetation coverage on regional water balance in the nonhumid regions of
771 China. *Water Resources Research*, 45: W00A14.

772 Yang, D.W., Sun, F.B., Liu, Z.T., Cong, Z.T., & Lei, Z.D., 2006. Interpreting the
773 complementary relationship in non-humid environments based on the Budyko
774 and Penman hypotheses. *Geophysical Research Letters*, 33(18): L18402.

775 Yang, H.B., Yang, D.W., Lei, Z.D., & Sun, F.B., 2008. New analytical derivation of the
776 mean annual water-energy balance equation. *Water Resources Research*, 44(3):
777 W03410.

778 Yang, L., Feng, Q., Yin, Z., Wen, X., Si, J., Li, C., & Deo, R.C., 2017. Identifying
779 separate impacts of climate and land use/cover change on hydrological
780 processes in upper stream of Heihe River, Northwest China. *Hydrological*
781 *Processes*, 31(5): 1100-1112.

782 Yang, T., Wang, C., Chen, Y., Chen, X., & Yu, Z., 2015. Climate change and water
783 storage variability over an arid endorheic region. *Journal of Hydrology*, 529:
784 330-339.

785 Ye, S., Li, H.-Y., Li, S., Leung, L.R., Demissie, Y., Ran, Q., & Blöschl, G., 2015.
786 Vegetation regulation on streamflow intra-annual variability through adaption
787 to climate variations. *Geophysical Research Letters*, 42(23): 10307-10315.

788 Ye, S., Li, H.Y., Li, S., Leung, L.R., Demissie, Y., Ran, Q., & Blöschl, G., 2016.
789 Vegetation regulation on streamflow intra-annual variability through adaption
790 to climate variations. *Geophysical Research Letters*, 42(23): 10307-10315.

791 Yuan, W., Liu, S., Liu, H., Randerson, J.T., Yu, G., & Tieszen, L.L., 2010. Impacts of
792 precipitation seasonality and ecosystem types on evapotranspiration in the
793 Yukon River Basin, Alaska. *Water Resources Research*, 46: W02514.

794 Zeng, R., & Cai, X., 2015. Assessing the temporal variance of evapotranspiration
795 considering climate and catchment storage factors. *Advances in Water*
796 *Resources*, 79: 51-60.

797 Zeng, R., & Cai, X., 2016. Climatic and terrestrial storage control on
798 evapotranspiration temporal variability: Analysis of river basins around the
799 world. *Geophysical Research Letters*, 43(1): 185-195.

800 Zha, T., Barr, A.G., van der Kamp, G., Black, T.A., McCaughey, J.H., & Flanagan, L.B.,
801 2010. Interannual variation of evapotranspiration from forest and grassland
802 ecosystems in western Canada in relation to drought. *Agricultural and Forest*
803 *Meteorology*, 150(11): 1476-1484.

804 Zhang, D., Cong, Z., Ni, G., Yang, D.,&Hu, S., 2015. Effects of snow ratio on annual
805 runoff within the Budyko framework. *Hydrology and Earth System Sciences*,
806 19(4): 1977-1992.

807 Zhang, D., Liu, X., Zhang, Q., Liang, K.,&Liu, C., 2016a. Investigation of factors
808 affecting intra-annual variability of evapotranspiration and streamflow under
809 different climate conditions. *Journal of Hydrology*, 543: 759-769.

810 Zhang, D., Liu, X., Zhang, L., Zhang, Q., Gan, R.,&Li, X., 2020. Attribution of
811 Evapotranspiration Changes in Humid Regions of China from 1982 to 2016.
812 *Journal of Geophysical Research-Atmospheres*, 125(13): e2020JD032404.

813 Zhang, L., Dawes, W.R. and Walker, G.R., 2001. Response of mean annual
814 evapotranspiration to vegetation changes at catchment scale. *Water Resources*
815 *Research*, 37(3): 701-708.

816 Zhang, S., Yang, H., Yang, D.,&Jayawardena, A.W., 2016b. Quantifying the effect of
817 vegetation change on the regional water balance within the Budyko framework.
818 *Geophysical Research Letters*, 43(3): 1140-1148.

819 Zhang, Y., Luo, Y., Sun, L., Liu, S., Chen, X.,&Wang, X., 2016c. Using glacier area
820 ratio to quantify effects of melt water on runoff. *Journal of Hydrology*, 538:
821 269-277.

822 Zhou, S., Yu, B., Huang, Y., & Wang, G., 2015. The complementary relationship and
823 generation of the Budyko functions. *Geophysical Research Letters*, 42(6):
824 1781-1790.